Article

TRANSPARENT PROCESS

EMBO reports

SPATA2 promotes CYLD activity and regulates TNF-induced NF-κB signaling and cell death

Lisa Schlicher[1,2,3], Manuela Wissler[1,‡], Florian Preiss[1,2,‡], Prisca Brauns-Schubert[1,2,‡], Celia Jakob[1], Veronica Dumit[4], Christoph Borner[1,2,3], Joern Dengjel[3,4,†] & Ulrich Maurer[1,2,3,*]

Abstract

K63- and Met1-linked ubiquitylation are crucial posttranslational modifications for TNF receptor signaling. These non-degradative ubiquitylations are counteracted by deubiquitinases (DUBs), such as the enzyme CYLD, resulting in an appropriate signal strength, but the regulation of this process remains incompletely understood. Here, we describe an interaction partner of CYLD, SPATA2, which we identified by a mass spectrometry screen. We find that SPATA2 interacts via its PUB domain with CYLD, while a PUB interaction motif (PIM) of SPATA2 interacts with the PUB domain of the LUBAC component HOIP. SPATA2 is required for the recruitment of CYLD to the TNF receptor signaling complex upon TNFR stimulation. Moreover, SPATA2 acts as an allosteric activator for the K63- and M1-deubiquitinase activity of CYLD. In consequence, SPATA2 substantially attenuates TNF-induced NF-κB and MAPK signaling. Conversely, SPATA2 is required for TNF-induced complex II formation, caspase activation, and apoptosis. Thus, this study identifies SPATA2 as an important factor in the TNF signaling pathway with a substantial role for the effects mediated by the cytokine.

Keywords apoptosis; CYLD; HOIP; SPATA2; TNF
Subject Categories Autophagy & Cell Death; Post-translational Modifications, Proteolysis & Proteomics
DOI 10.15252/embr.201642592 | Received 21 April 2016 | Revised 4 July 2016 | Accepted 5 July 2016 | Published online 25 July 2016
EMBO Reports (2016) 17: 1485–1497

Introduction

Non-degradative ubiquitylation is a crucial posttranslational modification for signaling through the TNF receptor 1 (TNFR1). Upon TNF ligation to its receptor, K63-linked and M1-linked (linear) ubiquitylation is mediated by ubiquitin ligases, which are recruited to the TNFR1 signaling complex (TNF-RSC), such as TRAF2/5, cIAP-1 and cIAP-2, and LUBAC [1–4]. Upon stimulation of the TNFR1, the generation of K63-linked ubiquitin chains results in the recruitment of TAB 2 or TAB 3, and thereby the kinase TAK1, as well as the LUBAC complex [4–6]. LUBAC is composed of the components SHARPIN, HOIL-1, and the enzyme HOIP, the latter providing the E3 Ligase activity. So far, LUBAC is the only known ubiquitin ligase which is able to generate M1-linked ubiquitin chains [7–9]. Together, K63-linked and linear ubiquitylation of TNF-RSC constituents creates a platform for the activation of the IKK (IκB kinase) complex and the MAP kinases like MKK6. These kinases mediate NF-κB and AP1 transcription factor activation and thereby inflammatory cytokine expression [10].

The ubiquitylation in the TNF-RSC is counter-regulated by deubiquitinases (DUBs) such as CYLD, A20, and OTULIN. Thereby, DUB activity can modify the assembly and the disassembly of the complex, respectively, and influence the strength and the outcome of TNFR signaling. Among these DUBs, the deubiquitinase CYLD is unique, as it has been shown to hydrolyze K63-linked ubiquitin chains as well as M1-linked ubiquitin chains, thereby attenuating TNFR-induced NF-κB signaling [11–18].

Upon TNFR1 stimulation, CYLD is recruited to the TNF-RSC by the LUBAC complex through the interaction with HOIP. This requires the peptide: N-glycanase/UBA or UBX-containing protein (PUB) domain of HOIP, but it is not clear whether the interaction of HOIP and CYLD is direct or not [16]. The M1-specific deubiquitinase OTULIN also interacts with LUBAC through the HOIP's PUB domain [19,20]. However, in contrast to CYLD, OTULIN is not recruited to the TNF-RSC [16]. In addition, the binding of CYLD and OTULIN to HOIP was shown to be mutually exclusive, while the reason for this is not understood [16].

Within hours after TNFR1 stimulation, a second complex, originating from the TNF-RSC, is forming, termed TNFR complex IIa. This complex consists of TRADD, RIPK1, FADD, caspase-8, and cFLIP and can serve as a platform to activate the initiator caspase-8. The protein cFLIP, which represents a caspase-8 homologue lacking protease activity, is transcriptionally induced upon intact NF-κB signaling [21]. cFLIP hetero-dimerizes with caspase-8, thereby preventing maturation and the pro-apoptotic activity of caspase-8 [22].

1 Institute of Molecular Medicine and Cell Research, Albert-Ludwigs-University Freiburg, Freiburg, Germany
2 Spemann Graduate School of Biology and Medicine (SGBM), Albert-Ludwigs-University of Freiburg, Freiburg, Germany
3 BIOSS, Centre for Biological Signaling Studies, Freiburg, Germany
4 Core Facility Proteomics, Center for Biological Systems Analysis, Freiburg, Germany
*Corresponding author. Tel: +49 761 203 9632; E-mail: ulrich.maurer@mol-med.uni-freiburg.de
†Present address: Department of Biology, University of Fribourg, Fribourg, Switzerland
‡These authors contributed equally to this work

However, an alternative route to TNF-mediated cell death exists, which is not controlled by NF-κB signaling. Instead, it requires the kinase activity of RIPK1 and is mediated by a complex termed TNFR complex IIb, which forms, for example, upon inhibition of cIAP1/2 [23]. RIPK1, in its ubiquitylated form, serves independently of its kinase activity as a scaffold in complex I. Deubiquitylation of RIPK1 was described to be mediated by CYLD, and this is thought to result in the formation of complex IIb consisting of RIPK1, FADD, and caspase-8, mediating caspase-8 activation [11,24]. Thus, in the context of cell death regulation, the deubiquitinase activity of CYLD plays a central role, as CYLD was demonstrated to be required for TNF-induced cell apoptosis and necroptosis [25]. The regulation of CYLD activity itself within the TNF-RSC, however, remains elusive.

The opposite effect on cell death was observed for the LUBAC component HOIP. Mice with a homozygous deletion of HOIP exhibit mid-gestation embryonic lethality, which is mediated by the TNFR1, and HOIP knockout mouse embryonic fibroblasts (MEFs) are prone to TNF-induced cell death [26].

The protein SPATA2 (spermatogenesis-associated protein 2) was initially shown to be highly expressed in testicular Sertoli cells, and these early reports suggested SPATA2 to play a role in spermatogenesis [27,28]. More recently, the *Spata2* locus was discussed to be involved in the predisposition for psoriasis [29,30].

During ongoing studies on the regulation of the activity of CYLD, we have identified SPATA2 as a CYLD-interacting protein. Here, we examine how SPATA2 affects TNF-induced signaling processes such as NF-κB and MAPK activation as well as TNF-mediated cell death.

We show that SPATA2 interacts with CYLD and HOIP, mediating the recruitment of CYLD to the TNF-RSC. We demonstrate that SPATA2 enhances the DUB activity of CYLD and that it thereby attenuates NF-κB and MAPK activation by TNF. Moreover, we show that SPATA2 is required for TNF-induced cell death.

Results

SPATA2 represents an interaction partner of CYLD

To explore the regulation of CYLD, we performed a SILAC mass spectrometry experiment, in order to identify novel interaction partners of CYLD, potentially impacting on its regulation. $CYLD^{-/-}$ MEFs were infected with retrovirus encoding FLAG-CYLD or were left uninfected as a control, followed by a labeling of the two different populations with the respective isotopes. The cells were then treated with TNF, subjected to a FLAG-IP, and after mixing the two conditions, the CYLD interactome was analyzed (Fig 1A). Among a number of identified interactors, we found the by far highest heavy/light ratio for the protein SPATA2 (spermatogenesis-associated protein 2), identifying it as a promising candidate as a novel interaction partner of CYLD (Fig 1B).

We first aimed at confirming the interaction between CYLD and SPATA2. Consistent with the results obtained by SILAC-MS, FLAG-tagged full-length CYLD, expressed in 293T cells, co-immunoprecipitated endogenously expressed SPATA2. The interaction with SPATA2 was also observed by immunoprecipitation of a FLAG-tagged C-terminal fragment of CYLD (CYLD 581–956), whereas an N-terminal fragment of CYLD (CYLD 1–581) did not interact with SPATA2 (Fig 1C). This interaction was also confirmed using $CYLD^{-/-}$ MEFs expressing FLAG-CYLD. Again, an anti-FLAG antibody co-immunoprecipitated endogenous SPATA2 (Fig 1D). The substantial enrichment of SPATA2 by co-immunoprecipitation with CYLD is consistent with a high affinity interaction.

In a reverse approach, we expressed FLAG-SPATA2 in 293T cells and, in line with previous experiments, we were able to detect a co-immunoprecipitation of endogenous CYLD. A construct lacking the C-terminal part of SPATA2, but retaining the N-terminus including the PUB domain of the protein, co-immunoprecipitated CYLD to a similar extent. This demonstrated that SPATA2 binds CYLD via the N-terminal part of SPATA2, which contains the PUB domain of SPATA2 (Fig 1E).

Together, these data indicate that SPATA2 and CYLD interact via the C-terminus of CYLD and the N-terminus of SPATA2.

SPATA2 interacts with HOIP and is recruited to the TNF-RSC

The LUBAC component HOIP was recently shown to recruit CYLD to the TNF-RSC, and the CYLD-HOIP interaction was shown to require the PUB domain of HOIP, as the N102A or N84A/Y93A PUB domain mutants of HOIP exhibited a largely reduced interaction with CYLD [16,31].

As SPATA2 interacts with CYLD, we postulated that SPATA2 is the bridging factor between CYLD and HOIP. We therefore tested whether SPATA2 interacts with HOIP. Indeed, we found that FLAG-HOIP co-immunoprecipitated with SPATA2 (Fig 2A). As shown previously for CYLD, the interaction of SPATA2 and HOIP also depended on an intact PUB domain of HOIP, as a PUB domain mutant, $HOIP^{N102A}$, exhibited a largely reduced interaction with SPATA2 (Fig 2A).

The M1-specific deubiquitinase OTULIN, which has been shown to also interact with the PUB domain of HOIP, requires a PUB interaction motif (PIM) for this association [19,20]. We tested the possibility that the interaction of SPATA2 and HOIP also depends on a PIM in SPATA2. We observed that SPATA2 contains a region with similarity to the OTULIN PIM and generated a SPATA2 PIM mutant in analogy to the OTULIN PIM Y56A mutation (which compromises the interaction of OTULIN with HOIP), by generating a $SPATA2^{Y338A}$ mutant [19,20]. As shown in Fig 2B, this SPATA2 mutant exhibited largely reduced binding to HOIP, while the interaction with CYLD was not affected. Together, these results demonstrate that SPATA2 interacts via a PUB interaction motif (PIM) with the PUB domain of HOIP.

OTULIN was also found to interact with HOIP through HOIP's PUB domain [16,19,20,31,32]. However, the binding of CYLD and OTULIN to HOIP was shown to be mutually exclusive, and while CYLD is recruited to the TNF-RSC by HOIP upon TNFR1 ligation, OTULIN is not [16]. As both SPATA2 and OTULIN interact with HOIP depending on HOIP's PUB domain, we asked whether SPATA2 and OTULIN compete for binding to HOIP.

We co-expressed FLAG-tagged HOIP with increasing amounts of SPATA2. Strikingly, when we analyzed endogenous OTULIN, which co-immunoprecipitated with HOIP, we found that high expression of SPATA2 abrogated the binding of OTULIN to HOIP (Fig 2C). This indicates that it is the competition of SPATA2 and OTULIN, which underlies the mutual exclusive binding of CYLD and OTULIN to the LUBAC complex. Consistently, a direct interaction of SPATA2 and OTULIN did not take place (Fig 2D).

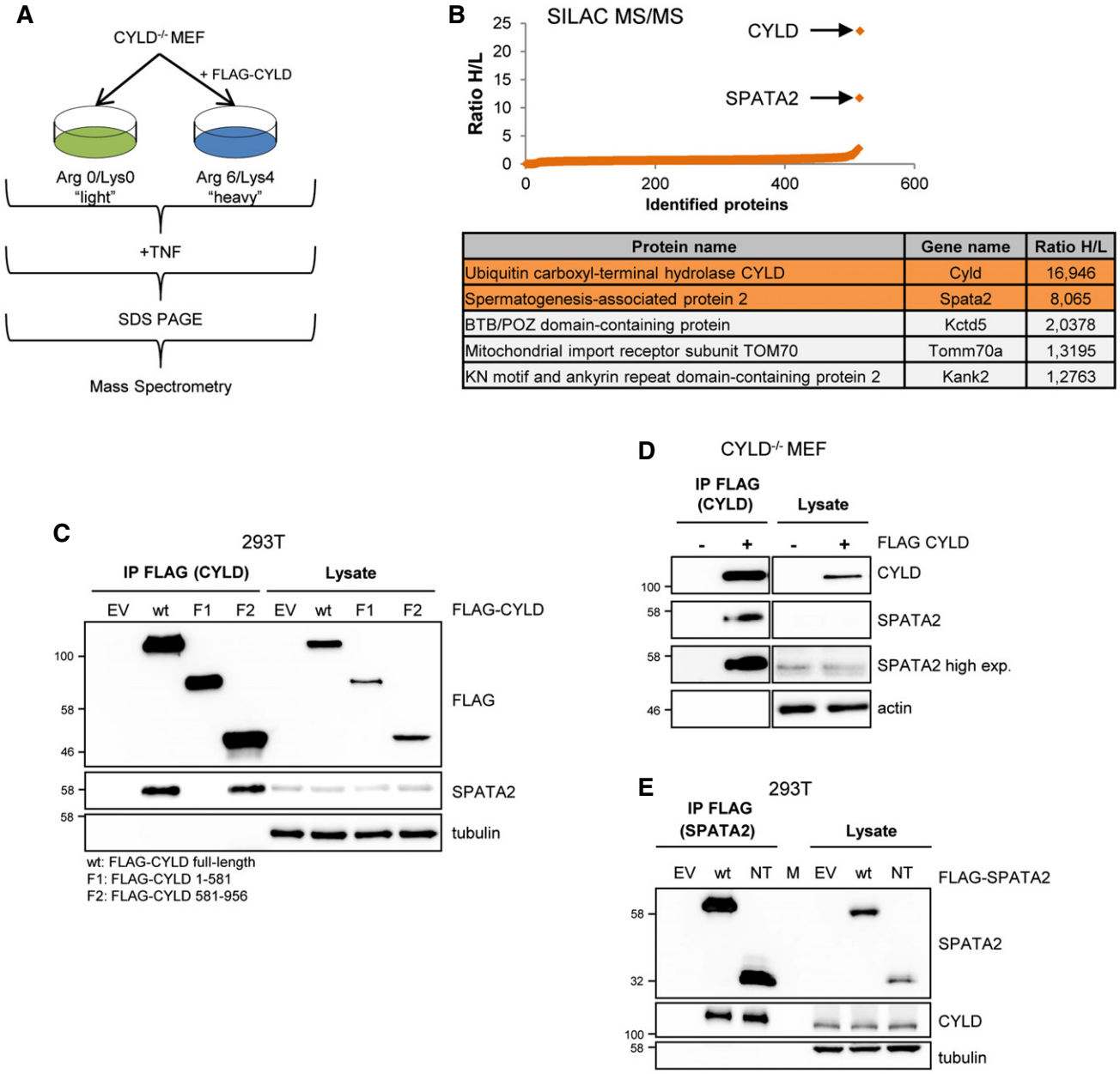

Protein name	Gene name	Ratio H/L
Ubiquitin carboxyl-terminal hydrolase CYLD	Cyld	16,946
Spermatogenesis-associated protein 2	Spata2	8,065
BTB/POZ domain-containing protein	Kctd5	2,0378
Mitochondrial import receptor subunit TOM70	Tomm70a	1,3195
KN motif and ankyrin repeat domain-containing protein 2	Kank2	1,2763

Figure 1. Interaction of CYLD and SPATA2.

A Differentially SILAC-labeled CYLD$^{-/-}$ cells and CYLD$^{-/-}$ cells expressing FLAG-CYLD were treated with mTNF (10 ng/ml). Purified FLAG-CYLD protein complexes were combined 1:1 and analyzed by LC-MS/MS.

B Heavy/light ratio for ~500 proteins identified in the screen. SPATA2 stands out with a substantially elevated H/L ratio. Each dot represents a protein.

C 293T cells were transfected with empty vector (EV), a vector encoding FLAG-tagged full-length CYLD (wt), or constructs encoding FLAG-tagged CYLD fragments 1–581 (F1) lacking the C-terminus, or 581–956 (F2) lacking the N-terminus, as indicated, followed by FLAG-IP. The blot was probed with antibodies recognizing SPATA2, FLAG, and tubulin. Endogenous SPATA2 was co-immunoprecipitated to comparable levels by CYLD and the C-terminal CYLD protein fragment, containing the USP domain.

D CYLD$^{-/-}$ MEFs were infected with retrovirus encoding FLAG-CYLD as indicated and CYLD was purified by FLAG-IP. The blot was probed with antibodies recognizing CYLD, SPATA2, and actin.

E 293T cells were transfected with empty vector (EV), a vector encoding FLAG-tagged full-length SPATA2, or a construct encoding the FLAG-tagged N-terminal part of SPATA2 (NT), as indicated, followed by FLAG-IP. The blot was probed with antibodies recognizing CYLD, SPATA2, and tubulin. M, marker lane.

SPATA2 itself also contains a PUB domain, and we asked whether this PUB domain contributes to the interaction with CYLD. In analogy to the HOIP PUB domain N102A mutant, we generated a SPATA2^{F108A} mutant, which exhibited no detectable binding to CYLD anymore (Fig 2E). Thus, the PUB domain of SPATA2 is required for the interaction with CYLD.

Together, these data suggest that SPATA2 is a bridging protein between HOIP and CYLD. As HOIP recruits CYLD to the TNF-RSC,

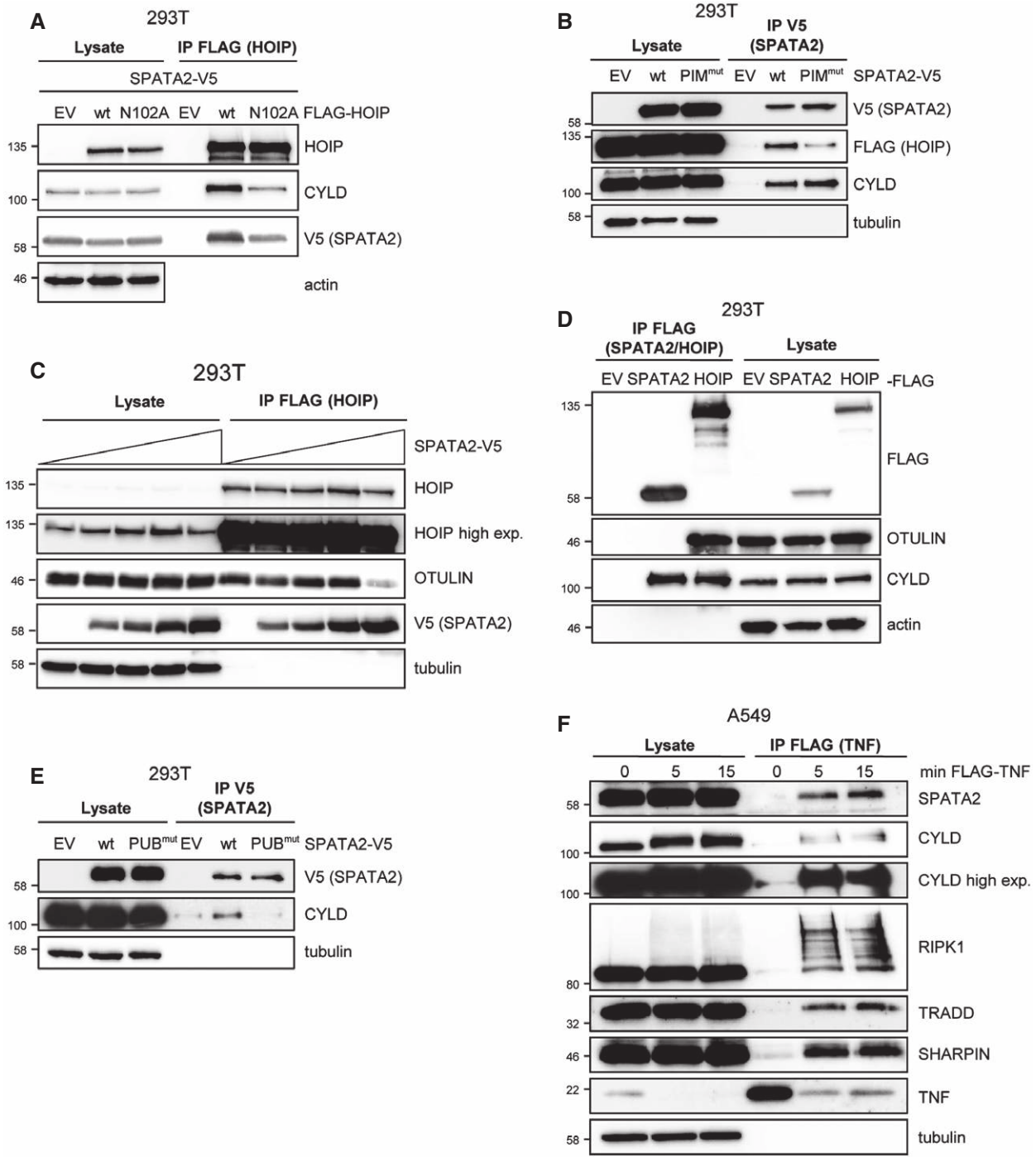

Figure 2. Interaction of HOIP and SPATA2 and recruitment of SPATA2 to the TNF-RSC.

A 293T cells were transfected with a vector encoding V5-tagged full-length SPATA2, along with empty vector (EV), a vector encoding FLAG-tagged HOIP wild-type (wt) or a vector encoding a FLAG-tagged PUB domain mutant of HOIP (N102A). After FLAG-IP, the blot was probed with antibodies recognizing HOIP, CYLD, V5, and actin.

B 293T cells were transfected with a vector encoding FLAG-tagged HOIP along with either empty vector, V5-tagged SPATA2 (wt) or a V5-tagged PIM mutant of SPATA2 (PIM^{mut}). After V5 IP, the blot was probed with antibodies recognizing FLAG, CYLD, V5, and tubulin.

C 293T cells were transfected with a vector encoding FLAG-tagged HOIP and increasing amounts of V5-tagged SPATA2. After FLAG-IP, the blot was sequentially probed with antibodies recognizing OTULIN, HOIP, V5, and tubulin.

D 293T cells were transfected with empty vector, FLAG-SPATA2, or FLAG-HOIP. After FLAG-IP, the blot was probed with antibodies recognizing OTULIN, CYLD, FLAG, and actin.

E 293T cells were transfected with empty vector, V5-tagged SPATA2 (wt), or a V5-tagged PUB domain mutant of SPATA2 (PUB^{mut}). After V5 IP, the blot was probed with antibodies recognizing CYLD, V5 and tubulin.

F A549 cells were treated with FLAG-hTNF (2 μg/ml) for the indicated time. The purified TNF-RSC was sequentially probed with antibodies recognizing SPATA2, CYLD, RIPK1, TRADD, SHARPIN, TNF, and tubulin as indicated.

SPATA2 should also be recruited to the TNF-RSC upon TNF stimulation. To test this, we stimulated A549 cells with FLAG-tagged TNF, followed by FLAG-IP of the receptor complex, at various time points. We found that SPATA2 was recruited with similar kinetics to the TNF-RSC as TRADD, RIPK1, SHARPIN, and CYLD (Fig 2F). This finding identifies SPATA2 as a component of the TNF-RSC.

The recruitment of CYLD to the TNF-RSC requires SPATA2

We further analyzed the role of SPATA2 as a bridging factor of CYLD and HOIP, by exploring whether it mediates the recruitment of CYLD to the TNF-RSC, which was previously shown to be HOIP dependent [16].

To address this question, A549 cells expressing CRISPR/Cas9, targeting SPATA2, were generated. These cells were treated with FLAG-tagged TNF, followed by FLAG-IP of the receptor complex at various time points. As shown in Fig 3A, CYLD recruitment to the TNF-RSC was compromised to the same extent as the recruitment of SPATA2 in cells which were infected with CRISPR/Ca9 targeting SPATA2. This indicated that SPATA2 mediates the interaction between CYLD and HOIP. Importantly, the recruitment of HOIP and SHARPIN to the TNF-RSC was not affected upon SPATA2 reduction (Fig 3A).

Likewise, MEFs lacking SPATA2 were generated by the CRISPR/Cas9 system, targeting *Spata2*, and clones with frameshift mutations, incompatible with productive protein expression, on both *Spata2* alleles were selected (Fig EV1A–C). Control cells were generated using a CRISPR/Cas9 system targeting luciferase. Upon treatment with FLAG-tagged TNF, followed by FLAG-IP of the receptor complex, CYLD recruitment to the TNF-RSC was increased only in the presence of SPATA2 corroborating the results we had obtained with A549 cells (Fig 3B).

Linear ubiquitylation was reported to be the predominant linkage type in the TNFR signaling pathway [33]. For this reason, and because CYLD is capable of counteracting M1-linked ubiquitylation, we specifically asked whether the absence of SPATA2-dependent recruitment of CYLD to the TNF-RSC results in increased M1-ubiquitylation on the TNF-RSC [14,15]. We tested this possibility using an antibody which is specific for M1-ubiquitin chains [34]. Indeed, upon stimulation and isolation of the TNF-RSC with FLAG-HA-tagged TNF, the complexes from SPATA2 knockout cells exhibited increased M1-ubiquitylation (Fig 3B).

Taken together, SPATA2 is required for CYLD recruitment to the TNF-RSC, which was previously shown to depend on HOIP [16]. Along with the finding that SPATA2 interacts with HOIP, dependent on its PIM, these data indicate that SPATA2 is the bridging factor between CYLD and HOIP for the recruitment of CYLD to the TNF-RSC.

Thus, in the absence of SPATA2, the loss of CYLD recruitment results in an increased ubiquitylation of the TNF-RSC. In consequence, SPATA2 would be expected to attenuate TNF-RSC signaling.

SPATA2 promotes the M1- and K63-specific DUB activity of CYLD

In principle, the absence of SPATA2, and therefore, the lack of CYLD recruitment to the TNF-RSC, would explain the increased M1-ubiquitylation we observed. However, we considered the possibility that the strong direct interaction of SPATA2 and CYLD could

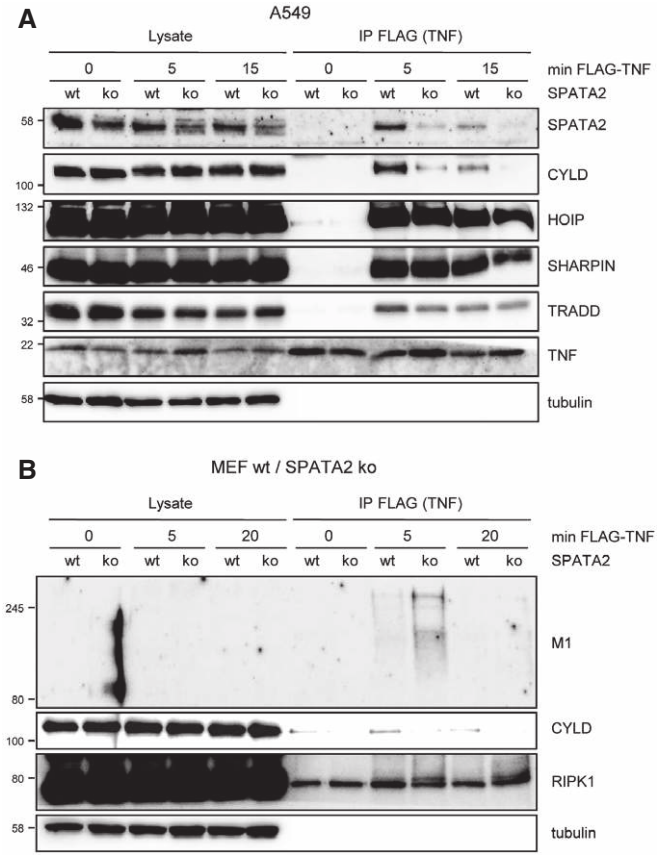

Figure 3. SPATA2-dependent recruitment of CYLD to the TNF-RSC.

A A549 cells were infected to express a CRISPR/Cas9 system targeting luciferase (as control, indicated wt) or the *SPATA2* gene (ko). Mixed cell cultures were treated with FLAG-hTNF (2 μg/ml) for the indicated time. The purified TNF-RSC was sequentially probed with antibodies recognizing SPATA2, CYLD, HOIP, SHARPIN, TRADD, TNF, and tubulin as indicated.

B MEFs were infected to express a CRISPR/Cas9 system targeting luciferase (wt) or the *Spata2* gene (ko). Single clones were generated, which were treated with FLAG-hTNF (2 μg/ml) for the indicated time. The purified TNF-RSC was sequentially probed with antibodies recognizing M1-linked ubiquitin, CYLD, RIPK1, and tubulin as indicated.

have effects on the enzymatic activity of CYLD. CYLD had been shown previously to cleave M1- and K63-, but not K48-linked ubiquitin chains [14,15]. We tested this hypothesis in a DUB activity assay by combining recombinant M1-, K63-, and K48-linked diubiquitin with purified FLAG-CYLD, co-expressed with or without SPATA2, to assess CYLD DUB activity.

We first retrovirally expressed FLAG-CYLD^{wt} or the inactive mutant FLAG-CYLD^{C598A} in CYLD$^{-/-}$ MEFs. These cells were infected with retrovirus encoding SPATA2, or control retrovirus. FLAG-CYLD was isolated by FLAG-IP and, as expected, SPATA2 co-purified with CYLD. The association did not depend on the enzyme activity of CYLD, as the inactive mutant FLAG-CYLD^{C598A} also co-immunoprecipitated SPATA2 (Fig 4A–C). The purified proteins were then combined with M1-, K63-, or K48-linked diubiquitin substrate. As expected, and consistent with data from others, wild-type CYLD mediated proteolysis of the M1- and K63-linked diubiquitin, while the inactive CYLD^{C598A} mutant did not [14]. When assaying the

DUB activity of FLAG-CYLD, which had been expressed in the presence of co-introduced SPATA2, we consistently observed an increased loss of the band representing diubiquitin, while the band representing mono-ubiquitin gained intensity (Fig 4A and B). In contrast, and consistent with previous findings by others, CYLD did not process K48-linked diubiquitins, and this was not influenced by the presence or absence of SPATA2 [14,15] (Fig 4C).

Together, these data indicate that SPATA2 is not only required for CYLD recruitment to the TNF-RSC, but also promotes the M1- and K63-DUB activity of CYLD, which results in a reduction of ubiquitylation at the TNF-RSC.

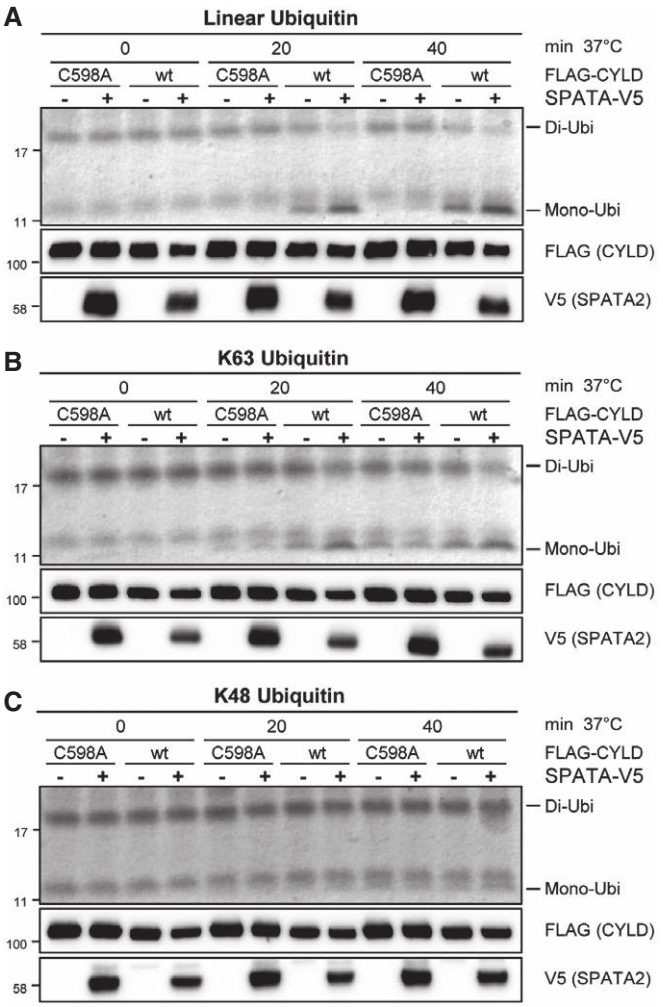

Figure 4. SPATA2 promotes CYLD DUB activity.

A–C FLAG-tagged CYLD or catalytically inactive FLAG-CYLD (C598A), respectively, was stably expressed in CYLD$^{-/-}$ MEFs, followed by infection with control retrovirus, or retrovirus encoding SPATA2, and purified by FLAG-IP. Purified CYLD or the inactive mutant was added to recombinant diubiquitin for 0, 20, or 40 min at 37°C as indicated. After electrophoresis, the gel was cut and the lower part was silver-stained to visualize mono- and diubiquitin, while the upper part was transferred to a membrane and probed for FLAG and V5. In (A), the experiment was done with M1-linked diubiquitin substrate; in (B), K63-linked diubiquitin substrate was subjected to the assay; and in (C), K48-linked diubiquitin substrate was analyzed.

SPATA2 attenuates TNF-induced NF-κB and MAPK activation

Linear and K63-linked ubiquitylation are essential for inflammatory cytokine signaling and the prevention of TNF-mediated cell death [7,23,26]. As CYLD has been shown to counteract linear and K63-linked ubiquitylation [14] and our data demonstrate that SPATA2 and CYLD might cooperate for this function, we explored whether SPATA2 has an influence on the activation of NF-κB and MAPK signaling by TNF. To answer this question, MEFs lacking and retaining SPATA2 were generated by use of the CRISPR/Cas9 system and analyzed for NF-κB and MAPK signaling. Upon treatment with TNF, SPATA2 knockout cells exhibited accelerated IκBα degradation as well as increased phosphorylation of p65, IκBα, JNK, p38, and ERK, as compared to control cells infected with a CRISPR/Cas9 construct targeting luciferase (Fig 5A).

This effect was also observed in mixed cell cultures (without generating single clones) expressing lentiCRISPRv2 targeting the *Spata2* gene, ruling out clonal effects as a reason for our observation [35]. Moreover, similar IκBα degradation as the one shown in Fig 5A was obtained clones from with different guide RNAs, targeting the *Spata2* gene (Fig EV2).

SPATA2 (then designated PD1) had been reported to be highly expressed in testicular Sertoli cells, which are capable of mediating inflammatory cytokine responses [27,36,37]. We therefore further investigated the functional role of SPATA2 in this cell type.

To investigate the role of SPATA2 for TNF-RSC-mediated NF-κB and MAPK activation, we knocked out SPATA2 by CRISPR/Cas9, as described before, in the 15P-1 Sertoli cell line (Fig EV3). Similar to the results obtained with MEFs, after stimulation with TNF, SPATA2 knockout cells exhibited increased phosphorylation of IκBα, p65, JNK, p38, and ERK, as well as accelerated degradation of IκBα (Fig 5B). Together, our data demonstrate that the loss of SPATA2 to the TNF-RSC results in increased NF-κB and MAPK signaling, indicating that the recruitment of SPATA2 to the TNF-RSC attenuates these pathways.

SPATA2 is required for TNF-induced cell death

Ubiquitylation in the TNF-RSC is critical for the prevention of cell death induced by TNF, as inhibition of K63-linked ubiquitylation by SMAC mimetics or the absence of linear ubiquitylation in HOIP-deficient cells entails rapid apoptosis upon TNF receptor stimulation [2,38–40]. Ubiquitylation in the TNF-RSC is also crucial for the recruitment of the TAB/TAK1 complex, the absence of which leads to rapid TNF-induced, RIPK1-dependent cell death [6,41].

Likewise, TNF-induced cell death in the absence of K63- or M1-linked ubiquitylation (in cells lacking cIAPs or HOIP), or the absence of TAK1 kinase activity depends on the enzymatic activity of RIPK1 [23,26,42].

We chose TAK1-deficient cells [42,43] as a model system for TNF-induced apoptosis. Using TAK1$^{-/-}$ MEFs, or control MEFs, a SPATA2 knockout was generated by CRISPR/Cas9, targeting the *Spata2* gene as described above (Fig EV1A and D). Upon treatment with TNF, caspase activity was assessed by probing for cleaved caspase-3 and PARP in *Spata2* wild-type and knockout cells. Strikingly, we found substantially reduced caspase-3 and PARP cleavage in cells lacking SPATA2. Necrostatin-1 suppressed caspase

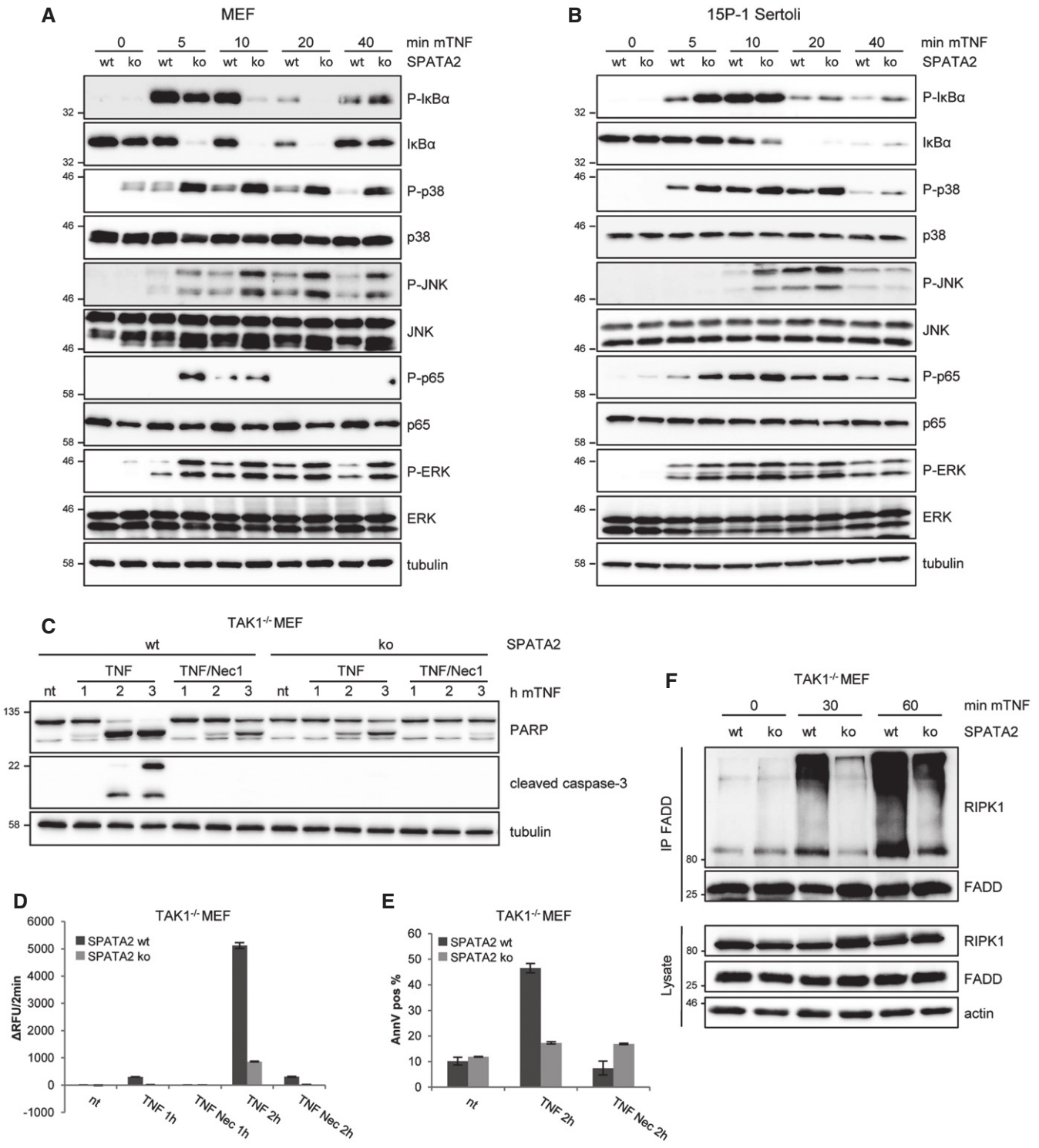

Figure 5.

activation, indicating that the death signal, promoted by SPATA2, is dependent on RIPK1 activity (Fig 5C).

We also analyzed caspase activity of TAK1$^{-/-}$ cells lacking or retaining SPATA2 after treatment with TNF, using the fluorogenic substrate DEVD-AMC. Consistent with the Western blot data as shown in Fig 5C, caspase activity was substantially reduced in cells lacking SPATA2 (Fig 5D). Likewise, the proportion of apoptotic, Annexin V-positive cells was substantially reduced in cells deficient for SPATA2 (Fig 5E). These results suggested that SPATA2 affects the formation of complex II. Therefore, we performed a FADD immunoprecipitation to isolate complex II using lysates from TAK1$^{-/-}$ cells lacking or retaining SPATA2 after treatment with

Figure 5. SPATA2 attenuates NF-κB and MAPK activation and promotes TNF-induced apoptosis.

A MEFs expressing CRISPR/Cas9 targeting luciferase (wt) or single clones generated from MEFs expressing CRISPR/Cas9 targeting the *Spata2* gene (ko) were treated with mTNF (10 ng/ml) as indicated. The blots were probed with antibodies recognizing P-IκBα, IκBα, P-p38, p38, P-JNK, JNK, P-p65, p65, P-ERK, ERK, and tubulin.

B 15P-1 Sertoli cells expressing CRISPR/Cas9 targeting luciferase (as control) or single clones generated from 15P-1 Sertoli cells expressing CRISPR/Cas9 targeting the *Spata2* gene were treated with mTNF (10 ng/ml) as indicated. The blots were probed with antibodies recognizing P-IκBα, IκBα, P-p38, p38, P-JNK, JNK, P-p65, p65, and tubulin.

C TAK1$^{-/-}$ MEFs were infected to express a CRISPR/Cas9 system targeting luciferase or the *Spata2* gene, from which single clones were generated. The cells were treated with mTNF (10 ng/ml) or mTNF along with necrostatin-1 (Nec-1) for 1–3 h as indicated. The blot was sequentially probed with antibodies recognizing PARP, cleaved caspase-3, and tubulin.

D The same cells as used in (C) were treated as before with TNF (10 ng/ml) or TNF along with necrostatin-1 (Nec-1) for 1 or 2 h as indicated. Caspase activity was determined using the fluorogenic substrate DEVD-AMC. A representative experiment is shown with error bars (representing SEM) referring to technical replicates.

E Cells from the experiment as shown in (D) were analyzed for apoptosis by Annexin V staining after 2 h. A representative experiment is shown with error bars (representing SEM) referring to technical replicates.

F Cells as described before were treated with mTNF (10 ng/ml) for the indicated time and lysates were subjected to immunoprecipitation with an anti-FADD antibody. The immunoprecipitates were subjected to Western blotting and probed for RIPK1, FADD, and actin.

TNF. We observed an interaction of RIPK1 with FADD in SPATA2 wild-type cells, while in SPATA2 ko cells, the interaction of RIPK1 with FADD was largely reduced, indicating an abrogated formation of the TNFR complex II (Fig 5F).

Thus, SPATA2 is required for proper complex II formation induced by TNF. Together, these data show that SPATA2, just like CYLD, promotes TNF-induced apoptosis, consistent with data previously reported by others [25].

Discussion

In this study, we identified SPATA2 as a constituent of the TNF-RSC, with important roles for the activation of both TNF-induced transcription activation and TNF-induced cell death.

Our finding that SPATA2 interacts with both HOIP and CYLD suggests the presence of a HOIP-SPATA2-CYLD complex, with SPATA2 being the bridging factor for the CYLD-HOIP interaction, which was reported previously by others [16,31,32]. Our data further show that, upon TNFR1 ligation, SPATA2 and CYLD are recruited together to the TNF-RSC, along with LUBAC, and that the recruitment of CYLD (but not LUBAC components) depends on SPATA2. In consequence, SPATA2 and CYLD recruitment leads to an attenuation of K63- and M1-ubiquitylation at the TNF-RSC.

We performed the SILAC-MS analysis, which detected the CYLD-SPATA2 interaction, upon treatment of the cells with TNF. However, the interaction data of SPATA2 and CYLD in 293T cells (in the absence of a TNF-RSC) and data from others, which showed that CYLD and HOIP interact already in the absence of TNFR stimulation, suggest that a preexisting HOIP-SPATA2-CYLD complex is recruited to the TNF receptor, upon activation of the receptor [16].

The M1-specific DUB OTULIN has been shown to also interact with HOIP, while the binding of CYLD and OTULIN to HOIP is mutually exclusive, and OTULIN is not recruited to the TNF-RSC [16]. Our data indicate that the competition of the respective PIM of SPATA2 and OTULIN for binding to the HOIP PUB domain underlies the mutual exclusive interaction of CYLD and OTULIN with HOIP.

As both OTULIN and SPATA2 are capable of binding to HOIP, this capacity alone cannot sufficiently explain the selective recruitment of SPATA and CYLD, but not OTULIN, to the TNF-RSC by LUBAC. As our data show that HOIP is recruited TNF-RSC in the absence of SPATA2, a possible explanation would be that the interaction of HOIP and OTULIN prevents HOIP from being recruited to the TNF-RSC.

Our finding that SPATA2 promotes CYLD activity suggests two ways as to how SPATA2 promotes CYLD activity at the TNF-RSC. First, SPATA2 recruits CYLD to the TNF-RSC via its direct interaction with HOIP, and secondly, it promotes CYLD activity within the complex through an allosteric activation of the DUB. This mechanism suggests a role of SPATA2 as an important modulator for appropriate innate immune signaling. Indeed, our data show that the loss of SPATA2 substantially promoted NF-κB and MAPK activation, and, strikingly, the absence of SPATA2 almost completely abrogated TNF-induced apoptosis.

In initial reports, the most abundant expression of SPATA2 was observed in Sertoli cells of the testes, leading to the interpretation of a role of SPATA2 for spermatogenesis. However, while speculative, our finding that SPATA2 attenuates NF-κB signaling is also compatible with the interpretation that the high expression levels of SPATA2 play a role for the immune privilege of testes. Interestingly, in one study on CYLD knockout mice, male CYLD$^{-/-}$ mice were reported to be infertile, which was explained by an absence of an early wave of germ cell apoptosis [11]. We speculate that it is also possible that unchecked innate immune signaling may have resulted in this phenotype, and SPATA2 knockout mice will be informative to further explore this hypothesis.

CYLD had been shown in a shRNA library screen with L929 cells to be required for apoptosis and necroptosis [25]. It is not clear how exactly CYLD promotes TNF-induced cell death, and the molecular mechanism how SPATA2 acts in this context remains to be determined as well. We show that complex II formation is compromised in the absence of SPATA2. CYLD had been shown to deubiquitylate RIPK1, which was suggested to promote TNF-induced cell death [11,24]. Thus, the cell death-promoting role of SPATA2, which we have observed, would be compatible with the enhanced the DUB activity of CYLD, resulting in RIPK1 deubiquitylation. However, in agreement with data from others, we find RIPK1 to be ubiquitylated in complex II, indicating that the role RIPK1 ubiquitylation plays for cell death prevention has yet to be clarified [42,44].

In conclusion, with SPATA2 we have identified a so far unknown important component in the TNF receptor signaling pathway. Since it is very likely that this protein plays also a role for other innate immunity signaling pathways such as TLR or NOD signaling, our

findings represent an important step toward a deeper understanding of the regulation of innate immunity.

Materials and Methods

Cell lines

HEK293T (ATCC), CYLD$^{-/-}$ MEFs (kindly provided by Ramin Massoumi, Lund University, Sweden), TAK1$^{-/-}$ and control wt MEFs (kindly provided by Yves Dondelinger and Mathieu Bertrand, Ghent University, Belgium), A549 (kindly provided by Florian Weinberg and Tilman Brummer, Freiburg University, Germany), and 15P-1 Sertoli cells (ATCC) were cultured in DMEM high glucose medium, supplemented with 10% fetal calf serum and 1% penicillin/streptomycin.

Retroviral transduction of CYLD$^{-/-}$ MEFs

To create CYLD$^{-/-}$ MEFs stably expressing FLAG-CYLD or the FLAG-tagged catalytic inactive mutant FLAG-CYLD^{C598A}, 293T cells were seeded in 78-cm^2 culture plates at 20% confluency for transfection to produce retroviral particles. The next day, cells were transfected with 3 μg pDEST-LTR-N-FLAG-HA-IRESpuro human FLAG-CYLD wt (Addgene 22544) or pDEST-LTR-N-FLAG-HA-IRESpuro human FLAG-CYLD C598A (created by using the QuickChange site-directed mutagenesis approach; Agilent) together with 3 μg Hit60 [45] and 3 μg pVSV-G (ClonTech) using PEI transfection. The following day, 5 mM butyrate (Sigma-Aldrich) was added to enhance expression, which was replaced by 4 ml media in the evening of the same day. The next day, viral supernatants were harvested and supplemented with 5 μg/ml polybrene (Sigma-Aldrich). After filtering the supernatant (0.45 μm), spinfection of the target cells was performed for 10 min at 400 *g*. The following day, selection of the cells was started using 4 μg/ml puromycin (Sigma-Aldrich) for 4 days. When required, these cells were then transduced with either a pLXIN control vector (BD Bioscience) or pLXIN human SPATA2-V5 [subcloned from pcDNA3.1-TOPO human SPATA2-V5 (vector description see below) in pLXIN vector (BD Bioscience)] in the same way as described above.

Generation of SPATA2 ko cell lines using lentiviral CRISPR Cas9

In order to generate SPATA2 ko cells, the lentiCRISPRv2 system was used as described by others [35]. Therefore, three lentiviral vectors were designed encoding for three different guide RNAs targeting different sequences of exon 1 within the *Spata2* gene. As control, a lentiviral vector was designed encoding for a guide RNA targeting luciferase sequence (Table 1). The production of lentiviral particles and subsequent infection and selection of target cells was performed as described for retroviral transduction above, using lentiviral packaging vectors. In this case 5 μg of lentiCRISPRv2 vector, 1.5 μg pMISSIONVSV-G (Sigma-Aldrich) and 3 μg pMISSION GAG POL (Sigma-Aldrich) were transfected using PEI. Infected cells were selected using 4 μg/ml puromycin for 4 days and mixed cultures were tested for Cas9 cleavage efficiency and NHEJ repair by performing a Surveyor assay. To do so, the exon 1 region of the *Spata2* gene was amplified by PCR (primers used: 5′: GGCACCAGT CAGAAGGGTAA; 3′: CCAGGATGTCCATTTTGAGC). Then, the Surveyor assay was performed according to manufacturers' protocol (Integrated DNA technologies) to detect mismatches due to mutations, indicating Cas9 nuclease cleavage and repair by NHEJ. Single cell clones were generated and shifts in the open reading frame generating a premature STOP codon were verified via sequencing. Clones with identical deletions on both alleles resulting in a premature STOP codon were chosen (Figs EV1 and EV3). Control cell lines transfected with luciferase control vector were used as mixed cultures. In case of the A549 cell line, mixed cultures were used, without generating single clones.

Table 1. Guide RNAs used for CRISPR/Cas9.

Guide RNA	Mouse *Spata2* gene	Human *SPATA2* gene
gRNA#1	ATCAGCCGAAATCGATATAA	ATCAGCCGGAATCGATAAAA
gRNA#2	TCAGCCGAAATCGATATAAA	CCGGCTGATCCAGTTCTATG
gRNA#3	CGCAGGTACTCATCGCTGCC	CGCAGGCACTCATCGCTGCC
Luciferase	ACCGCTCCGGCGAAGGCGAA	ACCGCTCCGGCGAAGGCGAA

Three different guide RNAs were used to generate CRISPR/Cas9 vectors, each targeting human or mouse *Spata2*. As a control, a CRISPR/Cas9 vector targeting *luciferase* was generated.

Immunoblotting and antibodies

Cells were seeded in 28-cm^2 culture plates at 30% confluency 1 day before treatment. For cell death experiments, cells were treated as indicated with necrostatin-1 (100 μM, ENZO, 1 h preincubation) and/or stimulated with mTNF (10 ng/ml, Peprotech) for the indicated time intervals.

Cells were washed before lysis using ice-cold PBS. Cell pellets were lysed on ice for 5 min using 30–100 μl of lysis buffer [20 mM Tris–HCl, pH 7.5, 150 mM NaCl, 1% Triton X-100, 5 mM EDTA, 1× protease inhibitor cocktail complete (Roche), MG132 (20 μM, Alexis Biochemicals), phosphatase inhibitor cocktail 1 (1:50, Sigma-Aldrich)]. Lysates were then centrifuged at 16,100 *g* for 10 min, 4°C. The supernatants were always kept on ice. Protein concentration was determined by using the Bradford reagent (Bio-Rad). Laemmli buffer was added to 40–70 μg of protein lysate and samples were boiled for 5 min at 95°C. In some cases, the same amount of lysate was loaded onto more than one gel to allow sequential probing with several antibodies. Proteins were separated on SDS–PAGE and transferred to nitrocellulose membranes. To detect proteins of interest, antibodies (Table 2) were diluted in 3% milk/TBS–Tween (0.1%).

Immunoprecipitation

For FLAG or V5 immunoprecipitation of FLAG-CYLD and FLAG- or V5-SPATA2 constructs expressed in 293T cells, the cells were seeded in 78-cm^2 culture plates at 25% confluency. The next day, cells were transfected with PEI reagent using the following plasmids (8 μg total DNA amount): pDEST-LTR-N-FLAG-HA-IRESpuro hCYLD (Addgene), pDEST-LTR-N-FLAG-HA-IRESpuro human CYLD fragment 1–581 (created by using QuickChange site-directed mutagenesis approach; Agilent), pDEST-LTR-N-FLAG-HA-IRESpuro human

Table 2. Antibodies used for Western blotting.

Antibody	Dilution	Product no.	Supplier
SPATA2	1:1,000	ARP59151_P050	BIOZOL
SPATA2	1:1,000	A302-493A	Bethyl Laboratories
FLAG M2	1:5,000	Monoclonal, F1804	Sigma
Tubulin	1:5,000	alpha clone YL1/2, MCA77G	AbDseroTEC
CYLD	1:1,000	D1A10, #8462	Cell Signaling Technology
Actin	1:20,000	#691000	MP Biomedicals
HOIP/RNF31	1:1,000	clone #875227, MAB8039	R&D systems
HOIP/RNF31	1:1,000	A303-560A	Bethyl Laboratories
V5	1:5,000	R960-25	Invitrogen
P-IκBα	1:1,000	14D4, #2859	Cell Signaling Technology
IκBα	1:500	C21, sc-371	Santa Cruz Biotechnology
P-p38	1:1,000	Thr180/Tyr182, D3F9, #4511	Cell Signaling Technology
p38	1:1,000	L53F8, #9228	Cell Signaling Technology
P-p65	1:1,000	S536, #3031	Cell Signaling Technology
p65	1:1,000	L8F6, #6965	Cell Signaling Technology
P-ERK	1:2,000	Thyr202/204, #9101	Cell Signaling Technology
ERK	1:400	K23, sc-94	Santa Cruz Biotechnology
P-JNK	1:1,000	Thr183/Tyr185, #9251	Cell Signaling Technology
JNK	1:1,000	#9252	Cell Signaling Technology
PARP	1:1,000	#9542	Cell Signaling Technology
cl. caspase-3	1:1,000	Asp175, # 9661	Cell Signaling Technology
OTULIN	1:300	ab151117	Abcam
TNFα	1:200	H-156, sc-8301	Santa Cruz Biotechnology
SHARPIN	1:1,000	14626-1-AP	Proteintech
TRADD	1:400	H278, sc-7868	Santa Cruz Biotechnology
M1-Ubi	1:1,000	1F11/3F5/Y102L	Genentech
RIPK1	1:1,000	D94C12, #3493	Cell Signaling Technology
FADD	1:1,000	1F7, ADI-AAM-212-E	ENZO
FADD	15 µl for IP	M19, sc-6036	Santa Cruz Biotechnology

CYLD fragment 581–956 (created by using QuickChange site-directed mutagenesis approach; Agilent), control vector pcDNA3.1/V5-His-TOPO (Invitrogen), pcDNA3.1 FLAG-hSPATA2 and hSPATA2-V5 were subcloned in pcDNA3.1-TOPO vector after PCR amplification from vector pF1KM hSPATA2 (Kazusa DNA Res. Inst.). In addition, for V5 immunoprecipitation the constructs pLXIN hSPATA2-V5 (subcloned from pcDNA3.1-TOPO human SPATA2-V5), pLXIN hSPATA2-V5 PIM^{mut} (Y338A), and hSPATA2-V5 PUB^{mut} (F108A) (created by using QuickChange site-directed mutagenesis approach; Agilent) were used. Twenty-four hours after transfection, cells were harvested and lysed in 300–800 µl lysis buffer and protein concentration was determined as described above. A 30–50 µg lysate aliquot was taken as input control and the remaining lysate (adjusted to the same protein concentration among different samples) was used for IP, rotated for 2 h at 4°C with FLAG M2 affinity gel (30 µl; Sigma-Aldrich) or anti-V5 agarose (30 µl; Sigma-Aldrich). Beads were washed three times with lysis buffer (see above). For elution of immune complexes, 30–40 µl lysis buffer was added to the beads containing either, for FLAG-IP: 3X FLAG® Peptide (150 ng/µl, Sigma-Aldrich) or for V5-IP: V5 peptide (10 µg/ml, Sigma-Aldrich) followed by incubation for 30 min, 4°C rotating. Laemmli buffer was added to the eluates and input controls, and SDS–PAGE analysis was performed as described above.

For FLAG immunoprecipitation of FLAG-CYLD stably expressed in $CYLD^{-/-}$ MEFs, cells were seeded in 78-cm^2 culture plates at 40% confluency. The next day, FLAG immunoprecipitation was performed as described above for transfected 293T cells.

For immunoprecipitation of the TNF-RSC, MEFs or A549 cells were seeded the day before at 35% confluency in 176-cm^2 culture plates. The next day, cells were stimulated with 2 µg/ml FLAG-HA-hTNF for the indicated time points. Cells were harvested and lysed as described above. To lysates of the unstimulated control samples, 0.20 µg/ml FLAG-HA-hTNF was added. Then, FLAG-IP and SDS–PAGE analysis was performed as described above.

For immunoprecipitation of TNFR complex II, $TAK1^{-/-}$ MEFs, lacking or retaining SPATA2, were seeded the day before at 35% confluency in 176-cm^2 culture plates. The next day, cells were stimulated with 10 ng/ml mTNF for 30 min or 60 min. Cells were harvested and lysed as described above. Lysates were incubated over night with 25 µl A Sepharose CL-4B (GE Healthcare) and 15 µl of anti-FADD (M-19, Santa Cruz Biotechnology). The next day, beads were washed three times with lysis buffer and then elution was performed by adding Laemmli buffer, followed by boiling at 95°C, 5 min. SDS–PAGE analysis was performed as described above. In some cases, the same amount of lysate was loaded onto more than one gel to allow sequential probing of several antibodies.

Cell death assays

For apoptosis quantification by FACS analysis, MEFs were seeded in duplicates in a 3.8-cm^2 culture plate at 30% confluency. The next day, for RIPK1 inhibition, cells were pretreated for 1 h with necrostatin-1 (100 µM, ENZO). Then, cells were stimulated with mTNF (10 ng/ml) for the indicated time points. Cells were harvested and washed once in Annexin binding buffer (10 mM Hepes, 140 mM NaCl, 2.5 mM $CaCl_2$, pH 7.4) followed by a staining for 15 min

within the same buffer using Alexa Fluor 647 Annexin V (Bio Legend, 200 ng/ml final concentration) in the dark. The fraction of Annexin V-positive cells was measured using a FACSCalibur (BD Bioscience).

Caspase-3 activity was measured by incubating whole cell lysates (20 μg in a volume of max. 40 μl) in duplicates with fluorogenic DEVD-AMC (60 μM, Enzo Life Science), adjusted to a final volume of 100 μl by adding caspase activity buffer (100 mM Hepes, pH 7.5, 10 mM DTT). When the substrate was added, fluorescence was measured immediately at 37°C for 30 min with a time interval of 2 min (Tecan Infinite M200 microplate reader). The slope of the linear regression was calculated to state the relative caspase activity.

DUB activity assay

To analyze CYLD catalytic activity dependent on SPATA2, CYLD$^{-/-}$ MEFs were used stably expressing FLAG-CYLD wt, or the catalytic inactive mutant C598A, respectively. These cells were each infected with retrovirus encoding SPATA2-V5 or empty vector, as described above. Cells were seeded in 176-cm^2 culture plates at 25% confluency. The next day, cells were harvested and FLAG-IP and elution was performed as described above, with the exception that the beads were washed after FLAG-IP as follows: one time washed with lysis buffer (see above), 2 times washed with PBS (adjusted to 400 mM NaCl), one time with PBS (150 mM NaCl) and in a final step with lysis buffer. Then, 10 μl eluate for each time point (0, 20, 40 min; 37°C) was incubated together with 1.5 μl 10× DUB buffer (500 mM NaCl, 500 mM Tris pH 7.4, 50 mM DTT) [46] and 100 ng diubiquitin (Ubiqbio) adjusted to a final volume of 15 μl using lysis buffer containing fresh protease inhibitors. The reaction was stopped by adding Laemmli buffer to the samples. Samples were run on a NuPage Novex 4–12% Bis-Tris protein gel using the corresponding NuPage MES SDS Running Buffer (Thermo Fisher Scientific). Ubiquitin cleavage was detected by silver staining (performed according to protocol, using SilverQuest™ Silver Staining kit, Life Technologies). Before silver staining, the upper half of the gel was cut and transferred to a membrane in order to probe with antibodies recognizing FLAG (CYLD) and V5 (SPATA2).

Mass spectrometry analysis

CYLD$^{-/-}$ MEFs and CYLD$^{-/-}$ MEFs stably expressing FLAG-CYLD wt were labeled for six cell doublings with either "light": L-arginine and L-lysine (Arg0/Lys0), or "heavy": L-arginine-$^{13}C_6$-$^{14}N_4$ and L-lysine-$^2H_4$ (Arg6/Lys4) SILAC DMEM media. SILAC-labeled cells were expanded up to two 176-cm^2 culture plates at 60% confluency for each cell type. Cells were treated with mTNF (20 ng/ml) for 20 min. After stimulation, cells were harvested (two plates of each condition were pooled) and lysed in 1 ml lysis buffer (see above), followed by FLAG immunoprecipitation as described above. Beads were washed three times using lysis buffer. In the final wash step, the beads of both conditions were combined and protein complexes were eluted by adding Laemmli buffer (containing 50 mM DTT) diluted in lysis buffer. For MS sample preparation and measurements, samples were prepared with 1 mM DTT for 5 min at 95°C and alkylated using 5.5 mM iodoacetamide for 30 min at 25°C. Protein mixtures were separated by SDS–PAGE (4–12% Bis-Tris mini gradient gel) and gel lanes were cut into 10 equal slices. Gel fractions were in-gel digested using trypsin (Promega) [47]. Digests were performed overnight at 37°C in 0.05 M NH_4HCO_3 (pH 8). About 0.1 μg of protease was used for each gel band. Peptides were extracted from the gel slices with ethanol and resulting peptide mixtures were processed on STAGE tips as described [48].

Samples analyzed by MS were measured on LTQ Orbitrap XL mass spectrometer (Thermo Fisher Scientific) coupled either to an Agilent 1200 nanoflow HPLC (Agilent Technologies) or an Eksigent NanoLC-ultra. HPLC-column tips (fused silica) with 75 μm inner diameter were self-packed with Reprosil-Pur 120 ODS-3 to a length of 20 cm. No pre-column was used. Peptides were injected at a flow of 500 nl/min in 92% buffer A (0.5% acetic acid in HPLC gradient grade water) and 2% buffer B (0.5% acetic acid in 80% acetonitrile, 20% water). Separation was achieved by a linear gradient from 10 to 30% of buffer B at a flow rate of 250 nl/min. The mass spectrometer was operated in the data-dependent mode and switched automatically between MS (max. of 1 × 10 ions) and MS/MS. Each MS scan was followed by a maximum of five MS/MS scans in the linear ion trap using normalized collision energy of 35% and a target value of 5,000. Parent ions with a charge states of $z = 1$ and unassigned charge states were excluded from fragmentation. The mass range for MS was m/z = 370–2,000. The resolution was set to 60,000. MS parameters were as follows: spray voltage 2.3 kV; no sheath and auxiliary gas flow; ion transfer tube temperature 125°C.

Software Xcalibur (Thermo Scientific) and Mascot Daemon version 2.4.0 (Matrix Science) were used for data acquisition and processing.

Expanded View for this article is available online.

Acknowledgements

We thank Ramin Massoumi for CYLD$^{-/-}$ MEFs, Yves Dondelinger and Mathieu Bertrand for TAK1$^{-/-}$ MEFs, Florian Weinberg and Tilman Brummer for cells, Robert Kelley (Genentech) for the M1Ubi-specific antibody, Henning Walczak for the construct to generate recombinant FLAG-HA-hTNF, Pavel Salavei for generating recombinant FLAG-HA-hTNF protein, Daniel Fisch for initial experiments, and Martina Weiss and Karin Neubert for excellent technical assistance. This study was supported by funding from the Centre for Biological Signalling Studies (BIOSS, EXC-294), Freiburg, Germany, and the Spemann Graduate School of Biology and Medicine (SGBM, GSC-4), Freiburg, Germany, both funded by the Excellence Initiative of the German Federal and State Governments, Germany and grant 112140 from the Deutsche Krebshilfe to UM.

Author contributions

LS and UM conceived the study and analyzed the data, assembled the figures and wrote the manuscript. LS, MW, FP, PB-S, and CJ performed experiments and analyzed the data. VD and JD performed mass spectrometry analyses. CB analyzed data and contributed to the writing of the manuscript.

Conflict of interest

The authors declare that they have no conflict of interest.

References

1. Vince JE, Pantaki D, Feltham R, Mace PD, Cordier SM, Schmukle AC, Davidson AJ, Callus BA, Wong WW-L, Gentle IE *et al* (2009) TRAF2 must

bind to cellular inhibitors of apoptosis for tumor necrosis factor (tnf) to efficiently activate nf-κb and to prevent tnf-induced apoptosis. *J Biol Chem* 284: 35906 – 35915

2. Bertrand MJM, Milutinovic S, Dickson KM, Ho WC, Boudreault A, Durkin J, Gillard JW, Jaquith JB, Morris SJ, Barker PA (2008) cIAP1 and cIAP2 facilitate cancer cell survival by functioning as E3 ligases that promote RIP1 ubiquitination. *Mol Cell* 30: 689 – 700
3. Varfolomeev E, Goncharov T, Fedorova AV, Dynek JN, Zobel K, Deshayes K, Fairbrother WJ, Vucic D (2008) c-IAP1 and c-IAP2 are critical mediators of tumor necrosis factor alpha (TNFalpha)-induced NF-kappaB activation. *J Biol Chem* 283: 24295 – 24299
4. Haas TL, Emmerich CH, Gerlach B, Schmukle AC, Cordier SM, Rieser E, Feltham R, Vince J, Warnken U, Wenger T *et al* (2009) Recruitment of the linear ubiquitin chain assembly complex stabilizes the TNF-R1 signaling complex and is required for TNF-mediated gene induction. *Mol Cell* 36: 831 – 844
5. Kanayama A, Seth RB, Sun L, Ea C-K, Hong M, Shaito A, Chiu Y-H, Deng L, Chen ZJ (2004) TAB 2 and TAB 3 activate the NF-kappaB pathway through binding to polyubiquitin chains. *Mol Cell* 15: 535 – 548
6. Wang C, Deng L, Hong M, Akkaraju GR, Inoue J, Chen ZJ (2001) TAK1 is a ubiquitin-dependent kinase of MKK and IKK. *Nature* 412: 346 – 351
7. Gerlach B, Cordier SM, Schmukle AC, Emmerich CH, Rieser E, Haas TL, Webb AI, Rickard JA, Anderton H, Wong WW-L *et al* (2011) Linear ubiquitination prevents inflammation and regulates immune signalling. *Nature* 471: 591 – 596
8. Ikeda F, Deribe YL, Skånland SS, Stieglitz B, Grabbe C, Franz-Wachtel M, van Wijk SJL, Goswami P, Nagy V, Terzic J *et al* (2011) SHARPIN forms a linear ubiquitin ligase complex regulating NF-κB activity and apoptosis. *Nature* 471: 637 – 641
9. Tokunaga F, Nakagawa T, Nakahara M, Saeki Y, Taniguchi M, Sakata S-I, Tanaka K, Nakano H, Iwai K (2011) SHARPIN is a component of the NF-κB-activating linear ubiquitin chain assembly complex. *Nature* 471: 633 – 636
10. Walczak H (2011) TNF and ubiquitin at the crossroads of gene activation, cell death, inflammation, and cancer. *Immunol Rev* 244: 9 – 28
11. Wright A, Reiley WW, Chang M, Jin W, Lee AJ, Zhang M, Sun S-C (2007) Regulation of early wave of germ cell apoptosis and spermatogenesis by deubiquitinating enzyme CYLD. *Dev Cell* 13: 705 – 716
12. Trompouki E, Hatzivassiliou E, Tsichritzis T, Farmer H, Ashworth A, Mosialos G (2003) CYLD is a deubiquitinating enzyme that negatively regulates NF-kappaB activation by TNFR family members. *Nature* 424: 793 – 796
13. Komander D, Lord CJ, Scheel H, Swift S, Hofmann K, Ashworth A, Barford D (2008) The structure of the CYLD USP domain explains its specificity for Lys63-linked polyubiquitin and reveals a B box module. *Mol Cell* 29: 451 – 464
14. Komander D, Reyes-Turcu F, Licchesi JDF, Odenwaelder P, Wilkinson KD, Barford D (2009) Molecular discrimination of structurally equivalent Lys 63-linked and linear polyubiquitin chains. *EMBO Rep* 10: 466 – 473
15. Ritorto MS, Ewan R, Perez-Oliva AB, Knebel A, Buhrlage SJ, Wightman M, Kelly SM, Wood NT, Virdee S, Gray NS *et al* (2014) Screening of DUB activity and specificity by MALDI-TOF mass spectrometry. *Nat Commun* 5: 4763
16. Draber P, Kupka S, Reichert M, Draberova H, Lafont E, de Miguel D, Spilgies L, Surinova S, Taraborrelli L, Hartwig T *et al* (2015) LUBAC-recruited CYLD and A20 regulate gene activation and cell death by exerting opposing effects on linear ubiquitin in signaling complexes. *Cell Rep* 13: 2258 – 2272
17. Brummelkamp TR, Nijman SMB, Dirac AMG, Bernards R (2003) Loss of the cylindromatosis tumour suppressor inhibits apoptosis by activating NF-kappaB. *Nature* 424: 797 – 801
18. Kovalenko A, Chable-Bessia C, Cantarella G, Israël A, Wallach D, Courtois G (2003) The tumour suppressor CYLD negatively regulates NF-kappaB signalling by deubiquitination. *Nature* 424: 801 – 805
19. Elliott PR, Nielsen SV, Marco-Casanova P, Fiil BK, Keusekotten K, Mailand N, Freund SMV, Gyrd-Hansen M, Komander D (2014) Molecular basis and regulation of OTULIN-LUBAC interaction. *Mol Cell* 54: 335 – 348
20. Schaeffer V, Akutsu M, Olma MH, Gomes LC, Kawasaki M, Dikic I (2014) Binding of OTULIN to the PUB Domain of HOIP Controls NF-kappa B signaling. *Mol Cell* 54: 349 – 361
21. Micheau O, Lens S, Gaide O, Alevizopoulos K, Tschopp J (2001) NF-kappaB signals induce the expression of c-FLIP. *Mol Cell Biol* 21: 5299 – 5305
22. Micheau O, Tschopp J (2003) Induction of TNF receptor I-mediated apoptosis via two sequential signaling complexes. *Cell* 114: 181 – 190
23. Wang L, Du F, Wang X (2008) TNF-alpha induces two distinct caspase-8 activation pathways. *Cell* 133: 693 – 703
24. O'Donnell MA, Legarda-Addison D, Skountzos P, Yeh WC, Ting AT (2007) Ubiquitination of RIP1 regulates an NF-kappaB-independent cell-death switch in TNF signaling. *Curr Biol* 17: 418 – 424
25. Hitomi J, Christofferson DE, Ng A, Yao J, Degterev A, Xavier RJ, Yuan J (2008) Identification of a molecular signaling network that regulates a cellular necrotic cell death pathway. *Cell* 135: 1311 – 1323
26. Peltzer N, Rieser E, Taraborrelli L, Draber P, Darding M, Pernaute B, Shimizu Y, Sarr A, Draberova H, Montinaro A *et al* (2014) HOIP deficiency causes embryonic lethality by aberrant TNFR1-mediated endothelial cell death. *Cell Rep* 9: 153 – 165
27. Graziotto R, Foresta C, Scannapieco P, Zeilante P, Russo A, Negro A, Salmaso R, Onisto M (1999) cDNA cloning and characterization of PD1: a novel human testicular protein with different expressions in various testiculopathies. *Exp Cell Res* 248: 620 – 626
28. Onisto M, Graziotto R, Scannapieco P, Marin P, Merico M, Slongo ML, Foresta C (2000) A novel gene (PD1) with a potential role on rat spermatogenesis. *J Endocrinol Invest* 23: 605 – 608
29. Capon F, Bijlmakers M-J, Wolf N, Quaranta M, Huffmeier U, Allen M, Timms K, Abkevich V, Gutin A, Smith R *et al* (2008) Identification of ZNF313/RNF114 as a novel psoriasis susceptibility gene. *Hum Mol Genet* 17: 1938 – 1945
30. Li X-L, Yu H, Wu G-S (2014) Investigating the genetic association of HCP5, SPATA2, TNIP1, TNFAIP3 and COG6 with psoriasis in Chinese population. *Int J Immunogenet* 41: 503 – 507
31. Takiuchi T, Nakagawa T, Tamiya H, Fujita H, Sasaki Y, Saeki Y, Takeda H, Sawasaki T, Buchberger A, Kimura T *et al* (2014) Suppression of LUBAC-mediated linear ubiquitination by a specific interaction between LUBAC and the deubiquitinases CYLD and OTULIN. *Genes Cells* 19: 254 – 272
32. Hrdinka M, Fiil BK, Zucca M, Leske D, Bagola K, Yabal M, Elliott PR, Damgaard RB, Komander D, Jost PJ *et al* (2016) CYLD limits Lys63- and Met1-linked ubiquitin at receptor complexes to regulate innate immune signaling. *Cell Rep* 14: 2846 – 2858
33. Xu M, Skaug B, Zeng W, Chen ZJ (2009) A ubiquitin replacement strategy in human cells reveals distinct mechanisms of IKK activation by TNFalpha and IL-1beta. *Mol Cell* 36: 302 – 314
34. Matsumoto ML, Dong KC, Yu C, Phu L, Gao X, Hannoush RN, Hymowitz SG, Kirkpatrick DS, Dixit VM, Kelley RF (2012) Engineering and structural

characterization of a linear polyubiquitin-specific antibody. *J Mol Biol* 418: 134 – 144

35. Sanjana NE, Shalem O, Zhang F (2014) Improved vectors and genome-wide libraries for CRISPR screening. *Nat Methods* 11: 783 – 784
36. Riccioli A, Starace D, Galli R, Fuso A, Scarpa S, Palombi F, De Cesaris P, Ziparo E, Filippini A (2006) Sertoli cells initiate testicular innate immune responses through TLR activation. *J Immunol* 177: 7122 – 7130
37. Wu H, Shi L, Wang Q, Cheng L, Zhao X, Chen Q, Jiang Q, Feng M, Li Q, Han D (2016) Mumps virus-induced innate immune responses in mouse Sertoli and Leydig cells. *Sci Rep* 6: 19507
38. Varfolomeev E, Blankenship JW, Wayson SM, Fedorova AV, Kayagaki N, Garg P, Zobel K, Dynek JN, Elliott LO, Wallweber HJA *et al* (2007) IAP antagonists induce autoubiquitination of c-IAPs, NF-kappaB activation, and TNFalpha-dependent apoptosis. *Cell* 131: 669 – 681
39. Vince JE, Wong WW-L, Khan N, Feltham R, Chau D, Ahmed AU, Benetatos CA, Chunduru SK, Condon SM, McKinlay M *et al* (2007) IAP antagonists target cIAP1 to induce TNFalpha-dependent apoptosis. *Cell* 131: 682 – 693
40. Petersen SL, Wang L, Yalcin-Chin A, Li L, Peyton M, Minna J, Harran P, Wang X (2007) Autocrine TNFalpha signaling renders human cancer cells susceptible to Smac-mimetic-induced apoptosis. *Cancer Cell* 12: 445 – 456
41. Vanlangenakker N, Vanden Berghe T, Bogaert P, Laukens B, Zobel K, Deshayes K, Vucic D, Fulda S, Vandenabeele P, Bertrand MJM (2011) cIAP1 and TAK1 protect cells from TNF-induced necrosis by preventing RIP1/RIP3-dependent reactive oxygen species production. *Cell Death Differ* 18: 656 – 665
42. Dondelinger Y, Jouan-Lanhouet S, Divert T, Theatre E, Bertin J, Gough PJ, Giansanti P, Heck AJR, Dejardin E, Vandenabeele P *et al* (2015) NF-κB-independent role of IKKα/IKKβ in preventing RIPK1 kinase-dependent apoptotic and necroptotic cell death during TNF signaling. *Mol Cell* 60: 63 – 76
43. Sato S, Sanjo H, Takeda K, Ninomiya-Tsuji J, Yamamoto M, Kawai T, Matsumoto K, Takeuchi O, Akira S (2005) Essential function for the kinase TAK1 in innate and adaptive immune responses. *Nat Immunol* 6: 1087 – 1095
44. Dondelinger Y, Aguileta MA, Goossens V, Dubuisson C, Grootjans S, Dejardin E, Vandenabeele P, Bertrand MJM (2013) RIPK3 contributes to TNFR1-mediated RIPK1 kinase-dependent apoptosis in conditions of cIAP1/2 depletion or TAK1 kinase inhibition. *Cell Death Differ* 20: 1381 – 1392
45. Soneoka Y, Cannon PM, Ramsdale EE, Griffiths JC, Romano G, Kingsman SM, Kingsman AJ (1995) A transient three-plasmid expression system for the production of high titer retroviral vectors. *Nucleic Acids Res* 23: 628 – 633
46. Licchesi JDF, Mieszczanek J, Mevissen TET, Rutherford TJ, Akutsu M, Virdee S, El Oualid F, Chin JW, Ovaa H, Bienz M *et al* (2012) An ankyrin-repeat ubiquitin-binding domain determines TRABID's specificity for atypical ubiquitin chains. *Nat Struct Mol Biol* 19: 62 – 71
47. Shevchenko A, Tomas H, Havlis J, Olsen JV, Mann M (2006) In-gel digestion for mass spectrometric characterization of proteins and proteomes. *Nat Protoc* 1: 2856 – 2860
48. Rappsilber J, Mann M, Ishihama Y (2007) Protocol for micro-purification, enrichment, pre-fractionation and storage of peptides for proteomics using StageTips. *Nat Protoc* 2: 1896 – 1906